

# Regulating the Architectures of Hydrogen-Bonded Frameworks through Topological Enforcement

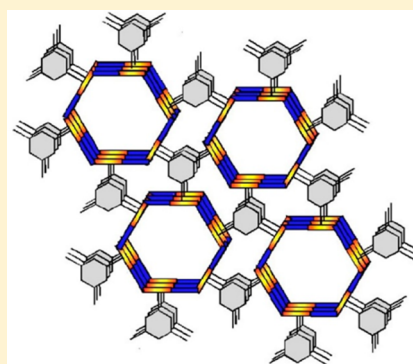
Yuzhou Liu,<sup>†</sup> Wenchang Xiao, Jin Ju Yi, Chunhua Hu, Sang-Jae Park,<sup>#</sup> and Michael D. Ward\*

The Department of Chemistry and the Molecular Design Institute, New York University, 100 Washington Square East, New York, New York 10003-6688, United States

**S** Supporting Information

**ABSTRACT:** The role of conformational flexibility in topological enforcement of several crystalline materials based on hydrogen-bonded two-dimensional guanidinium-sulfonate (GS) networks is demonstrated by using a series of organopolysulfonates that prompt the formation of either lamellar or cylindrical architectures. Whereas flexible organopolysulfonate linkers decorated with flexible arms self-assemble into lamellar architectures, rigid organopolysulfonates linkers enforce the formation of hydrogen-bonded cylinders with intercylinder spacing governed by the size of the linker. Specifically, hexagonal cylindrical structures generated from trisulfonates with three-fold molecular symmetry are the topological equivalent of the cylindrical hexagonal phases reported previously for guanidinium organomonosulfonate inclusion compounds, but neighboring cylinders are now connected through covalent nodes provided by the trisulfonates rather than dispersive interactions between the arene rings of the organomonosulfonates.

Organopolysulfonates with moderate conformational freedom, however, can generate both lamellar and cylindrical structures, depending on the guest molecules encapsulated by the host framework. These observations illustrate that the crystal architecture (i.e., lamellar vs cylindrical) and the shape of GS cylinders can be regulated in a predictable way by the molecular symmetries and conformational constraints of the organopolysulfonates building blocks.



## ■ INTRODUCTION

Since the discovery of urea inclusion compounds,<sup>1</sup> in which linear organic guests are confined within hydrogen-bonded one-dimensional channels of the urea host, many cylindrical crystalline inclusion compounds have been reported based on a variety of host frameworks, including those assembled from perhydrotriphenylene (PHTP),<sup>2</sup> tris(*o*-phenylenedioxy)cyclo-triphosphazene (TPP),<sup>3</sup> macrocycle bis-urea,<sup>4</sup> and dipeptides.<sup>5</sup> The formation of nanosized cylindrical channels is particularly interesting because of potential applications in gas separation/storage,<sup>6</sup> enhanced reaction selectivity,<sup>7</sup> and molecular conductivity.<sup>3</sup> Organic cylindrical structures have been achieved through hydrogen bonding as well as van der Waals interactions.<sup>8</sup> But reliable prediction and control of crystal architecture remains a central challenge in solid-state chemistry. Moreover, systematic modification of cylindrical hosts is rare, as even a seemingly innocent modification to the molecular constituents can lead to unpredictable changes in host architecture and often complete frustration of host framework formation.<sup>9</sup>

The realization of predictable and persistent host framework architectures requires design principles that employ directional forces that guide assembly of molecular constituents. Our laboratory and others have reported the design and construction of molecular frameworks built from two-dimensional quasi-hexagonal hydrogen-bonded networks of guanidinium (G) and sulfonate (S) groups of organomonosulfonates

and disulfonates.<sup>10–16</sup> Our laboratory has demonstrated the formation of crystalline hexagonal cylindrical host frameworks from guanidinium organomonosulfonates, with structural attributes reminiscent of hexagonal micelles (Figure 1).<sup>17,18</sup> These cylindrical structures can be depicted as a curled sheet comprising six GS ribbons, wherein the organic substituents on the sulfonate nodes protrude from the outer surface of the cylinders. The surface of the GS cylinder is not unlike that of a single-walled carbon nanotube (SWNT), which can be generated conceptually by curling of a graphene sheet.<sup>19</sup> A SWNT can adopt zigzag, armchair, or chiral configurations, depending on the direction and registry of the folding. Only the zigzag configuration has been observed previously for the GS cylinders, however.

The GS cylindrical structures were favored with respect to lamellar forms for disc-shaped guest molecules that fit comfortably within the cylinder, but the structure-directing influence of the guest molecule sometimes can be murky. For example, guanidinium 4-chlorobenzenesulfonate crystallizes in a lamellar host architecture with *m*-xylene guests, but the cylindrical host is observed for *o*-xylene guests. With *o*-xylene as a guest, 4-iodobenzenesulfonate and *p*-toluenesulfonate form a lamellar and cylindrical architecture, respectively. These observations demonstrate that solid-state structure design

Received: January 16, 2015

Published: March 2, 2015

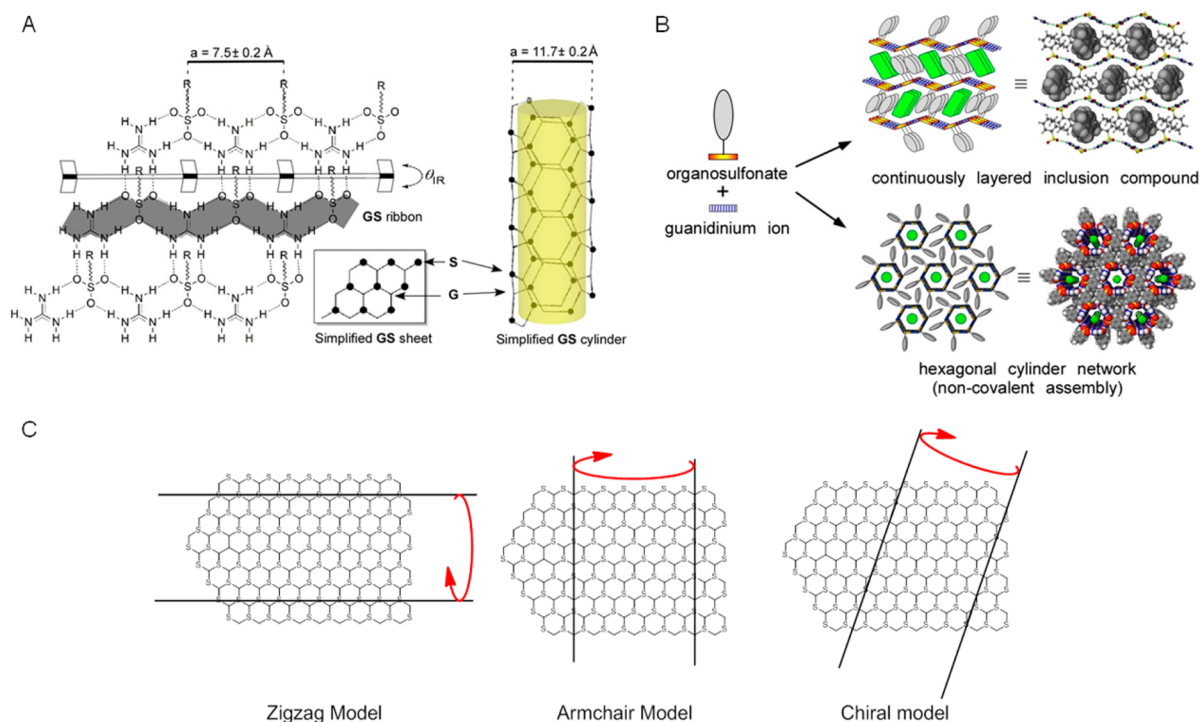


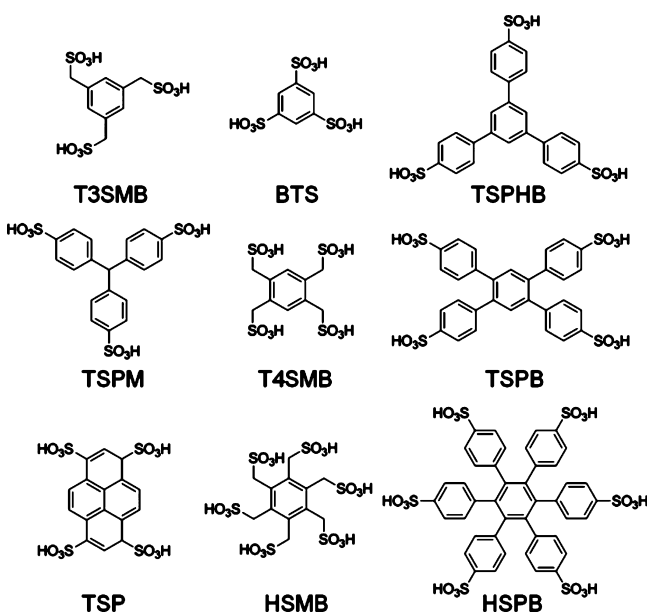
**Figure 1.** (A) Two-dimensional quasi-hexagonal GS hydrogen-bonded sheet and a simplified schematic of a GS cylinder. (B) Schematic representation of the noncovalent assembly of the lamellar and hexagonal cylindrical inclusion compounds with guanidinium organomonosulfonates. Guest molecules are indicated in green. (C) Three different ways to fold a GS sheet.

based on shape and size of the host constituents and guest molecules, in which assembly is guided by weak dispersive interactions, can be somewhat unpredictable even when based on a robust supramolecular hydrogen bond network.

Herein we report a series of GS frameworks built from organopolysulfonates that exhibit lamellar and cylindrical architectures depending on the degree of conformational flexibility (or conversely, rigidity) of the organic component. Whereas organopolysulfonates with flexible alkyl linkers form close-packed lamellar structures due to metric compatibility of

the sulfonate groups and their positions in the GS sheet, rigid organopolysulfonates frustrate the formation of lamellar structures and promote the formation of cylindrical structures through topological enforcement provided by the symmetry of the sulfonate groups. Specifically, hexagonal cylindrical structures generated from trisulfonates with three-fold molecular symmetry are the topological equivalent of the cylindrical hexagonal phases reported previously for guanidinium organomonosulfonate inclusion compounds, but neighboring cylinders are now connected through covalent nodes provided by the trisulfonates rather than dispersive interactions between the arene rings of the organomonosulfonates. Organopolysulfonates with moderate conformational flexibility, however, can organize as both lamellar and cylindrical structures, depending on the guest molecules. Moreover, the shape of the GS cylinders is affected by the symmetry of the polysulfonate. Trisulfonates with three-fold symmetry generate hexagonal-shaped cylinders mimicking the aforementioned cylindrical structures, while tetrasulfonates with two-fold symmetry form rectangular like channels. These examples validate the strategy of manipulating crystal architecture through directional hydrogen bonding.

#### Scheme 1



## RESULTS AND DISCUSSION

**Organotrissulfonates with Three-Fold Molecular Symmetry.** Guanidinium 1,3,5-trisulfonatomethylenebenzene ( $G_3$ T3SMB) crystallized in the  $R3c$  space group. Single crystal X-ray diffraction revealed a guest-free lamellar architecture, like that often observed for guanidinium organomonosulfonates. The three sulfonate substituents project in the same direction with respect to the benzene core such that the sulfonate triad is incorporated into the same GS sheet (Figure 2), thereby forming a “molecular basket” appended to the GS sheet through methylene “handles.” All the molecular baskets project

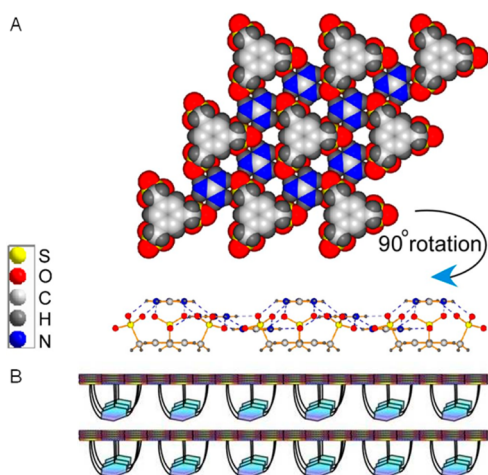


**Figure 2.** Packing modes of  $G_3T3SMB$  as viewed in directions perpendicular and parallel to the GS sheet (A) and schematic view of the molecular baskets in lamellar sheets (B).

from the same side of each sheet, and in the same direction for all sheets, generating polar alignment. Although these organotrisulfonates can be described as baskets, the free volume is negligible owing to the short sulfonate handles. This contrasts with metal complexes of the homologous benzene-1,3,5-tris(methylenephosphonic acid), wherein two handles connect one sheet and the third to the opposing sheet.<sup>20</sup> This different configuration may be attributed to the shorter phosphonate-phosphonate distance in the metal-phosphonate sheet motif (6.78 Å) compared with the 7.5 Å sulfonate-sulfonate in the GS sheet.

The guanidinium salts of 1,3,5-benzenetrisulfonate (BTS), tri(4-sulfophenyl)methane (TSPM), and 1,3,5-tri(4-sulfophenyl)benzene (TSPHB) crystallize in a cylindrical architecture ( $G_3BTS$  and  $G_3TSPHB$  in space group  $P6_3/m$ ;  $G_3TSPM$  in  $P6_3$ ). In these cases, the formation of a lamellar architecture is precluded by the symmetry and rigidity of the trisulfonates. Instead, these structures are the topological equivalent of the cylindrical hexagonal phases reported previously for guanidinium organomonosulfonate inclusion compounds, but neighboring cylinders are now connected through covalent nodes provided by the trisulfonates rather than dispersive interactions between the arene rings of the organomonosulfonates (Figure 3). The intercylinder spacing corresponds to the unit cell parameter  $a$ , increasing in the order for the sizes of the connectors  $G_3BTS$  (16.91 Å) <  $G_3TSPM$  (21.46 Å) <  $G_3TSPHB$  (23.86 Å). The hydrogen-bonding connectivity of the quasi-hexagonal GS sheet wrapping the cylinder surface was identical for the three compounds, with minor differences in the S...S distance along the major GS ribbon, which coincides with the cylinder axis (BTS = 7.585 Å; TSPHB = 7.443 Å; TSPM = 7.581 Å). These values are within the range of  $7.5 \pm 0.2$  Å typically observed for the quasi-hexagonal GS sheet in cylindrical and lamellar guanidinium mono- and disulfonates.

The covalent cylindrical frameworks include guest molecules in two kinds of void spaces, one inside the hydrogen-bonded cylinders and the other between the cylinders, the size of which depends on the organotrisulfonate linker. The framework void space, determined as a percentage based on the solvent accessible volume in the cylinders and between the cylinders (estimated using Platon)<sup>21</sup> was 54.4% for  $G_3BTS$ , 60.8% for

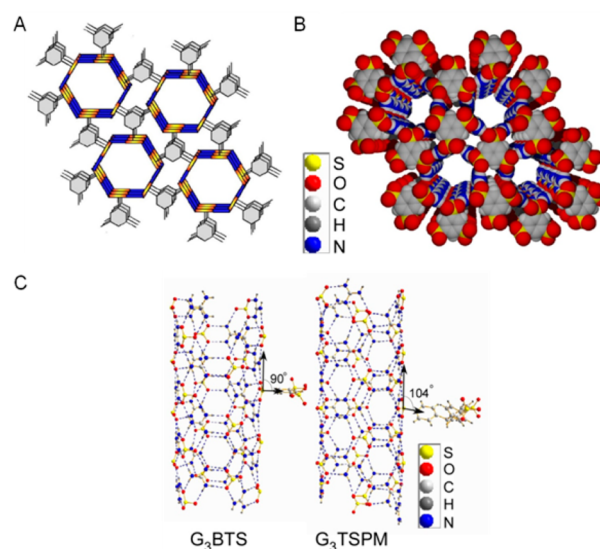


**Figure 3.** (A) Schematic representation of the covalent cylindrical architecture formed from a rigid tritopic linker. The yellow and blue bars indicate the sulfonate (S) and guanidinium (G) ions are depicted as yellow and blue, respectively. (B) Cylinder packing of  $G_3BTS$ . Methanol and 2,6-dichlorotoluene have been removed for clarity. (C) Comparison of the cylinder-sulfonate angles in  $G_3BTS$  and  $G_3TSPM$ , the latter illustrating the consequence of the pyramidal geometry of the TSPM linker that joins adjacent cylinders. Only one cylinder and one organosulfonate are depicted for simplicity. Further inspection of the three cylindrical structures reveals the presence of mirror symmetry in  $G_3BTS$  and  $G_3TSPHB$ .  $G_3TSPM$ , however, is polar due to the pyramidal geometry of the TSPM linker and the associated unsymmetrical hydrogen bonding of the guanidinium ion with sulfonate ions (C).

$G_3TSPM$ , 65.2% for  $G_3TSPHB$ , respectively. Unlike the cylindrical guanidinium organomonosulfonate inclusion compounds, the absence of any lamellar structures argues that formation of the cylindrical frameworks was guided more by the organotrisulfonate symmetry rather than templating by guests. Nonetheless, guests are required to promote and stabilize the low-density cylindrical frameworks. Crystallization does not occur in the absence of suitable guest molecules, and the resulting inclusion compounds become amorphous upon standing or when the guests are removed by heating (Table S3). Notably, guests included in the cylinders of the topologically equivalent cylindrical host frameworks realized from organomonosulfonates were largely simple substituted arenes, which formed  $\pi$ -stacks that were commensurate with the sulfonate-sulfonate distances along the cylinder direction. In the case of the  $G_3TSPM$ , however, it appears that the cylinders can incorporate nonaromatic guests and even longer guests such as cis-stilbene, suggesting more versatility as a consequence of the topological enforcement by covalent linkers. (Table S3).

Single crystals of  $G_3BTS(2,6\text{-dichlorotoluene})_3(\text{methanol})_2$ ,  $G_3TSPM(\text{mesitylene})_{3.67}$ , and  $G_3TSPHB(o\text{-xylene})_5(\text{methanol})_2$  afforded the best structural refinements among 14 host-guest combinations. Guest molecules were located within the cylinders and between cylinders in all cases. The refinement of  $G_3TSPM(\text{mesitylene})_{3.67}$  was sufficient to allow assignment of 2/3 of a mesitylene guest within the cylinder for every TSPM linker. The remaining three mesitylene guests were located between the cylinders, in cavities surrounding the linker. The structural refinements of

the other two compounds were not sufficient to assign the distribution of guest molecules.

**Organotetrasulfonates with Two-Fold Molecular Symmetry.** Guanidinium 1,2,4,5-tetrasulfatomethylene benzene ( $G_4T4SMB$ ) crystallized in a bilayer structure, space group  $P\bar{1}$ . The four sulfonate groups adopt an up–down–down–up configuration (Figure 4A), wherein 1,5 and 2,4

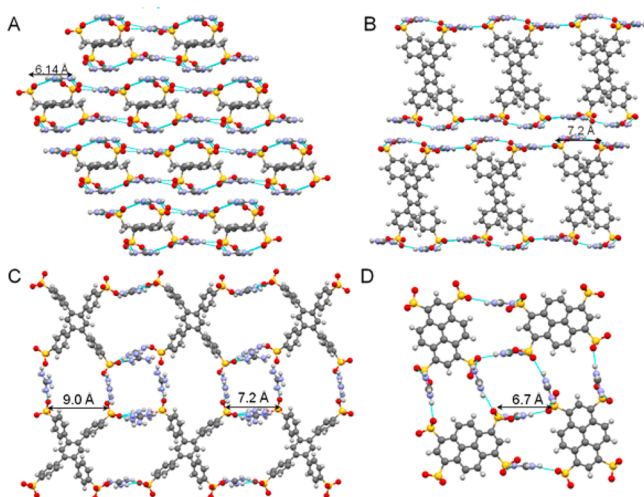


**Figure 4.** (A) Crystal structure of  $G_4T4SMB$ , viewed along the  $a$  axis. (B) Crystal structure of  $G_4TSPB$  (along the  $b$  axis) crystallized from water/acetone solution. Acetone guests have been removed for clarity. (C) Crystal structure of  $G_4TSPB$  (along the  $a$  axis) crystallized from a water/dioxane solution. Dioxane guests have been removed for clarity. (D) Crystal structure of  $G_4TSP$  (along the  $c$  axis) crystallized from a water/acetone solution. Acetone guests have been removed for clarity.

sulfonate pairs attach to opposite GS sheets. The absence of a 1,2/4,5 configuration can be attributed to the short S...S distances within these pairs compared with the requirements for insertion into the GS sheet. The S...S distance between sulfonates in the 1,5 pair (6.14 Å) approaches that of the typical S...S distance in the GS sheet ( $7.5 \pm 0.2$  Å), to the extent that these pairs can be accommodated by the quasi-hexagonal GS sheet, albeit with the G ions somewhat displaced out of the sheet plane. It seems reasonable to suggest that the flexible handles of  $T4SMB$  would allow a configuration in which 1,4 and 2,5 pairs would attach to opposite GS sheets, but this was not observed.

Compared with  $T4SMB$ , the 1,2,4,5-tetra(4-sulfonatophenyl)benzene ( $TSPB$ ) is much more constrained conformationally. Inspection of compounds in the Cambridge Structural Database (CSD, v. 5.35, 2013) containing  $TSPB^{4-}$  revealed that the S...S distance between 1,2 sulfonate pairs ranges from 6.8 to 8.6 Å, within reach of the 7.5 Å S...S distance required for the GS sheet in the lamellar architecture. Accordingly, guanidinium 1,2,4,5-tetra(4-sulfonatophenyl)benzene ( $G_4TSPB$ ) crystallized in space group  $P\bar{1}$  as a lamellar bilayer structure, with acetone guest molecules (Figure 4B). The S...S distance between the sulfonate groups in the 1,2 and 4,5 pairs is 7.2 Å, permitting insertion of each pair into opposing quasi-hexagonal GS sheets. The cross shape of  $TSPB$  molecules also shapes the free space inside the framework. Along the  $b$  direction, a series of hexagonal channels are defined by the arms of neighboring  $TSPB$  molecules, with three equivalents of acetone molecules included. Interestingly, our laboratory recently reported a different  $G_4TSPB$  framework when

crystallized from a water-dioxane mixture,<sup>22</sup> in which three crystallographically unique one-dimensional channels (Figure 4C) were filled with 5 equiv of dioxane molecules. The S...S distance between the 1,2-sulfonates in each  $TSPB$  molecule is 9.0 Å. This suggests that  $TSPB$  is more flexible than may be expected, enabling formation of either a lamellar or cylindrical architecture, depending on the guest molecules.

The conformationally rigid  $TSP^{4-}$  ion formed a guanidinium 1,3,6,8-tetrasulfonato-pyrene ( $G_4TSP$ ) framework, crystallizing exclusively in the space group of  $Pnmm$  with well-defined 6.7 Å wide channels flanked by four GS ribbons (Figure 4D). The framework also contained a second channel flanked by two GS ribbons and the edges of the pyrene units. Both channels are filled with one equivalent of acetone per  $TSP$ .

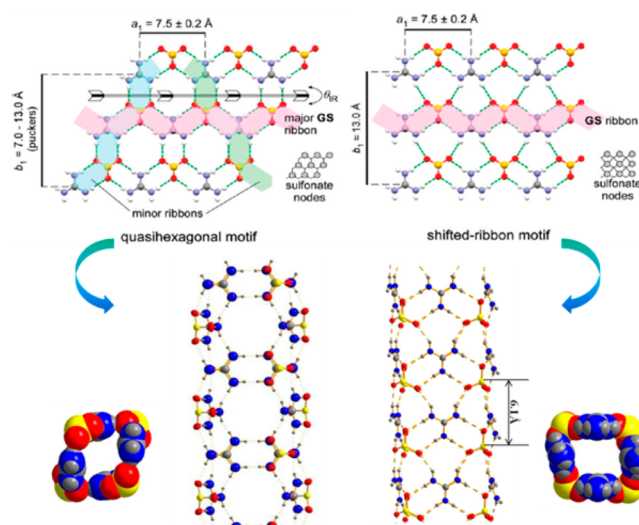


**Figure 5.** Left: Quasi-hexagonal hydrogen-bonded GS motif and the  $G_4TSP$  cylinder formed by this motif. Right: Shifted-ribbon GS motif and the  $G_4TSPB$  cylinder formed by this motif.

The four framework architectures generated from these tetrasulfonates reveal a trend from lamellar to cylindrical with increasing rigidity. Examination of the GS cylindrical frameworks reveals different GS hydrogen-bonded motifs. The  $G_4TSP$  cylinders emulate the zigzag folding of single-walled carbon nanotubes (SWNTs), whereas the  $G_4TSPB$  cylinders emulate the armchair configuration. The armchair configuration can be regarded as an extension of the “shifted ribbon” motif observed previously in some GS lamellar frameworks, but wrapped into a rectangular cylinder.<sup>23</sup> The inherent two-fold symmetry of host molecules is responsible for the shape of the rectangular cylinders, illustrating the potential for forming channels with shapes and sizes more complex than simple cylinders with circular cross sections.

**Organohexasulfonates with Three- and Six-Fold Molecular Symmetry.** The conformationally flexible guanidinium hexakisbenzenemethylsulfonate ( $G_6HSMB$ ) adopts a bilayer architecture, with 1,3,5 and 2,4,6 sulfonate triads attached to opposing quasi-hexagonal GS sheets (Figure 6). The configuration creates dome-shaped baskets, wherein the guanidinium ions sit above the arene ring, denoted here as a G-centered configuration, not unlike  $G_3T3SMB$  (see above). Like  $G_3T3SMB$ , the free volume inside the basket is negligible due to the short length of the sulfonate substituent.

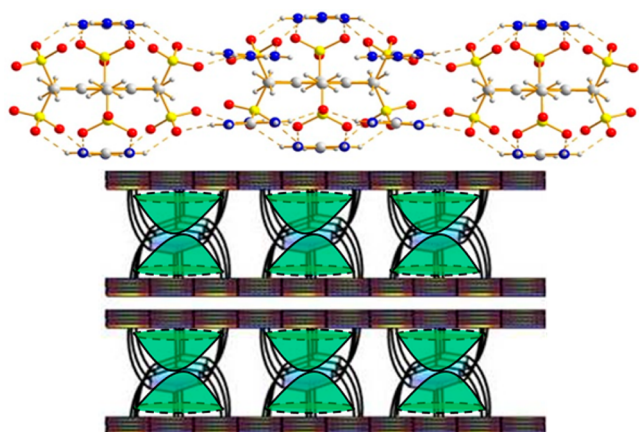


**Figure 6.** Upper panel: Packing in a layer of  $G_6HSMB$ . The 1,3,5 and 2,4,6 sulfonate triads attach to opposing quasi-hexagonal GS sheets. Color Code: carbon = gray; sulfur = yellow; oxygen = red; nitrogen = blue; hydrogen = black. Lower panel: Schematic view of the bilayer structure.

The cylindrical phase of  $G_4TSPB$  exhibits the armchair folding configuration, in contrast to the GS cylinders in the aforementioned  $G_3BTS$ ,  $G_3TSPHB$ ,  $G_3TSPM$ , and  $G_4TSP$  and previously reported guanidinium monosulfonates, which wrap by zigzag folding. The observation of the armchair configuration in  $G_4TSPB \cdot (dioxane)_5$  prompted us to consider whether the armchair motif could be achieved through rational design. The key difference between the zigzag and armchair configurations is the direction of the fold: the former results when the sheet curls transverse to the GS ribbons, and the latter results when the sheet curls parallel to the ribbon (Figure 1). The S...S distance is 12 Å in zigzag model but only 7.5 Å in the armchair mode. This suggests that the armchair folding would be most likely for rigid tri- and hexasulfonates equipped with intramolecular S...S distances near 7.5 Å. The intramolecular S...S distances in the rigid trisulfonates range from 5.442 Å for  $BTS$ , 10.281 Å for  $TSPM$ , to 12.924 Å for  $TSPHB$ , either too short or too long for the armchair configuration. A CSD search reveals S...S distances in hexa(4-sulfonatophenyl)benzene ( $HSPB^{6-}$ ) ranging from 6.8 to 8.6, however, with an average of 7.6, suggesting an possible candidate for a cylindrical structure with the armchair configuration in which the cylinders would have six-fold symmetry.<sup>24</sup> Growth of  $G_6HSPB$  by slow evaporation of an anhydrous methanol solution produced crystals with a needle-like morphology. The crystals were severely twinned, but crystal X-ray diffraction revealed armchair 2 nm-wide GS cylinders constructed from folding of the quasi-hexagonal motif, supported by 12 “spokes” emanating from columnar arrays of the  $HSPB^{6-}$  ions (Figure 7).

The free volume between the central arene rings of the  $HSPB$  plates is ca. 100 Å<sup>3</sup>, defined by a cavity that is isolated due to the interlocking of peripheral phenyl rings of neighboring plates. The cylinders are organized into hexagonal arrays. This packing is the reverse of that observed for guanidinium monosulfonate cylinders, which form hexagonal arrays as a consequence of interdigitated arene rings projecting from the exterior surface of the GS cylinder. The intramolecular S...S distance for each  $HSPB$  molecule is 7.504 Å, ideal for GS sheet formation. The distance between adjacent  $HSPB$  molecules along the tube is 5.53 Å (Figure 8).

As predicted, the  $(GS)_6$  cylinder in  $G_6HSPB$  adopts the armchair model, the only possible mode for this organo-

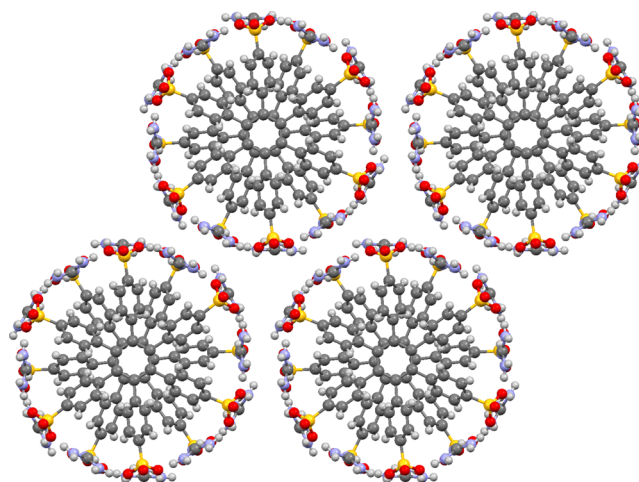


**Figure 7.** Packing schemes for  $G_6HSPB$ , in which the hexaphenylbenzene cores are surrounded by guanidinium sulfonate cylindrical layers. Methanol molecules, disordered in three directions, which forms hydrogen interactions with the hexaphenylbenzene columns are omitted for clarity.

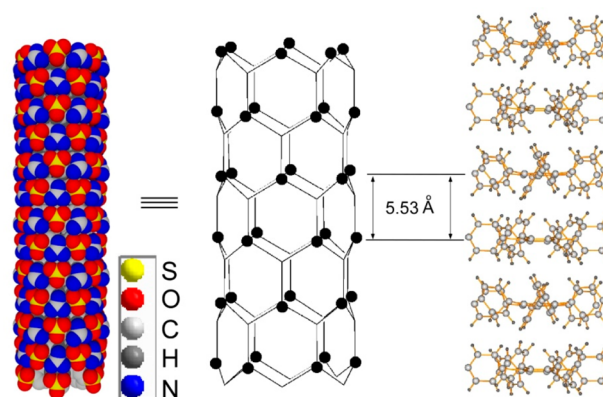


**Figure 8.** (left) Space-filled representation of zigzag hydrogen-bonding topology of the cylinders in  $G_6HSPB$  and (center) in simplified form, wherein the filled circles denote the sulfonate positions and the undecorated vertices the guanidinium positions. The stacking of the aromatic cores of  $HSPB^{6-}$  molecules illustrates the arrangement along the cylinder (right).

sulfonate. With the organic groups enclosed within the hydrogen-bonded cylinders, the zigzag or chiral model cannot support an intraribbon S...S distance of 7.5 Å perpendicular to the cylinder axis. The  $(GS)_6$  cylinder is chiral with a space group of  $P6$  due to the unsymmetrical hydrogen bonding between guanidinium and sulfonate ions along the cylinder.

## CONCLUSION

Capitalizing on the robust and persistent GS hydrogen-bonded network, the collection of solid-state structures here reveals a continuum of architectures resulting from the degree of conformational flexibility of polysulfonate building blocks. Whereas flexible organopolysulfonate linkers decorated with flexible arms self-assemble into lamellar architectures, rigid organopolysulfonate linkers enforce the formation of hydrogen-bonded cylinders with intercylinder spacing governed by the size of the linker. The principle of topological enforcement is very apparent from the observation of hexagonal cylindrical structures generated from trisulfonates with three-fold molec-

ular symmetry; these structures are the topological equivalent of the cylindrical hexagonal phases reported previously for guanidinium organomonosulfonate inclusion compounds, but neighboring cylinders are now connected through covalent nodes provided by the trisulfonates rather than dispersive interactions between the arene rings of the organomonosulfonates. Organopolysulfonates with moderate conformational freedom, however, can generate both lamellar and cylindrical structures, depending on the guest molecules encapsulated by the host framework. Like other GS compounds, there is no evidence for polymorphs or for architectural isomers having the same host–guest combination (from PXRD of batches of single crystals; Figures S11–S16). These observations illustrate that the crystal architecture (i.e., lamellar vs cylindrical) and the shape of GS cylinders can be regulated in a predictable way through control of the molecular symmetries and conformational constraints of the organopolysulfonates building blocks.

## EXPERIMENTAL SECTION

**Materials and General Procedures.** 1,3,5-benzenetrisulfonic acid (BTS), tri(4-sulfophenyl)methane (TSPM), 1,3,5-tri(4-sulfophenyl)benzene (TSPHB), 1,3,5-benzenetrimethylsulfonic acid (T3SMB), 1,2,4,5-tetrasulfonatomethylene benzene (T4SMB), hexakisbenzenemethylsulfonic acid (HSMB), and hexa(4-sulfophenyl) benzene (HSPB) were synthesized according to published procedures.<sup>25–30</sup> All chemicals were purchased from Sigma-Aldrich and used as received. The sulfonates were converted to the acid form by elution through an Amberlyst 36 (wet) ion-exchanged column. The respective guanidinium salts were precipitated from the acetone or acetone/methanol solution of sulfonic acid with guanidinium tetrafluoroborate, which was prepared by neutralization of guanidinium carbonate with tetrafluoroboric acid. The guanidinium salts were then dissolved in water or methanol with guest molecules, and single crystals suitable for X-ray diffraction analysis were grown by either slow evaporation or acetone diffusion into the solution. Infrared spectra of the single crystals were acquired with a PerkinElmer System 2000 FT-IR. Element analysis was performed on PerkinElmer 2400 Series II CHNS/O Elemental Analyzer.

**Preparation of G<sub>3</sub>T3SMB.** Slow evaporation of an aqueous solution of G<sub>3</sub>T3SMB afforded plate-shaped crystals. Elemental anal. calcd for C<sub>12</sub>H<sub>27</sub>O<sub>9</sub>S<sub>3</sub>N<sub>9</sub>: C 26.81, H 5.06, N 23.45. Found: C 26.77, H 4.74, N 23.45. IR: 3370 (vs), 3258 (m), 3198 (vs), 2933 (w), 2824 (w), 2769 (w), 2679 (w), 2232 (w), 1678 (vs), 1585 (m), 1458 (w), 1420 (w), 1258 (m), 1186 (s), 1126 (s), 1041 (s), 892 (w), 773 (m), 691 (m), 663 (m), 620 (m), 521 (s).

**Preparation of G<sub>3</sub>BTS-(2,6-dichlorotoluene)<sub>3</sub>(MeOH)<sub>2</sub>.** Layering of a methanol solution of G<sub>3</sub>BTS on 2,6-dichlorotoluene afforded needle-shaped crystals. Elemental anal. calcd for C<sub>32</sub>H<sub>47</sub>O<sub>11</sub>S<sub>3</sub>N<sub>9</sub>Cl<sub>6</sub>: C 36.86, H 4.54, N 12.09. Found: C 36.39, H 4.18, N 11.89. IR: 3368 (s), 3266 (m), 3200 (s), 1669 (vs), 1572 (m), 1436 (m), 1379 (w), 1203 (vs), 1106 (s), 1087 (m), 1034 (vs), 815 (s), 769 (s), 759 (s), 693 (m), 607 (m).

**Preparation of G<sub>3</sub>TSPHB-(o-xylene)<sub>3</sub>(MeOH)<sub>2</sub>.** Layering of a methanol solution of G<sub>3</sub>TSPHB on o-xylene afforded needle-shaped crystals. Elemental anal. calcd for C<sub>69</sub>H<sub>91</sub>O<sub>11</sub>S<sub>3</sub>N<sub>9</sub>: C 62.84, H 6.96, N 9.56. Found: C 62.50, H 6.93, N 9.41. IR: 3363 (s), 3261 (w), 3198 (s), 1671 (s), 1585 (m), 1496 (w), 1466 (w), 1384 (w), 1176 (s), 1126 (s), 1035 (s), 1007 (s), 823 (m), 742 (m), 707 (s), 620 (m).

**Preparation of G<sub>3</sub>TSPM-(mesitylene)<sub>3,6,7</sub>.** Layering of a methanol solution of G<sub>3</sub>TSPM on mesitylene afforded needle-shaped crystals. Elemental anal. calcd for C<sub>55</sub>H<sub>75</sub>O<sub>9</sub>S<sub>3</sub>N<sub>9</sub>: C 59.95, H 6.81, N 11.44. Found: C 58.36, H 6.85, N 11.36. IR: 3402 (s), 3261 (m), 3197 (s), 3017 (w), 2914 (w), 2853 (w), 2221 (s), 1673 (vs), 1606 (m), 1582 (m), 1472 (w), 1403 (w), 1378 (w), 1209 (s), 1176 (s), 1123 (s), 1035 (s), 1007 (s), 871 (w), 835 (m), 740 (m), 710 (s), 641 (s), 577 (m), 536 (m).

**Preparation of G<sub>4</sub>T4SMB.** Slow evaporation of an aqueous solution of G<sub>4</sub>T4SMB afforded well-defined plate-like crystals.

Elemental anal. calcd for C<sub>14</sub>H<sub>34</sub>O<sub>12</sub>S<sub>4</sub>N<sub>12</sub>: C 24.35, H 4.93, N 24.35. Found: C 24.97, H 4.83, N 24.76. IR: 3380 (w), 3258 (s), 3201 (w), 1677 (s), 1580 (m), 1216 (s), 1180 (s), 1095 (s), 1036 (s), 775 (s), 654 (w), 518 (s).

**Preparation of G<sub>4</sub>TSPB-(acetone)<sub>3</sub>.** Slow diffusion of acetone vapor into an aqueous solution of G<sub>4</sub>TSPB afforded plate-shaped crystals. Elemental anal. calcd for C<sub>43</sub>H<sub>60</sub>O<sub>15</sub>S<sub>4</sub>N<sub>12</sub>: C 46.40, H 5.40, N 15.11. Found: C 46.94, H 5.81, N 14.68. IR: 3408 (w), 3186 (w), 1666 (s), 1180 (m), 1126 (s), 1035 (s), 1008 (s), 833 (s), 754 (s), 661 (s).

**Preparation of G<sub>4</sub>TSPB-(dioxane)<sub>5</sub>.** Slow diffusion of dioxane vapor into an aqueous solution of G<sub>4</sub>TSPB afforded long block-shaped crystals. Elemental anal. calcd for C<sub>54</sub>H<sub>86</sub>O<sub>22</sub>S<sub>4</sub>N<sub>12</sub>: C 46.89, H 6.22, N 12.17. Found: C 47.31%, H 6.38%, N 12.05%. IR: 3368 (w), 3194 (w), 1663 (s), 1596 (w), 1475 (m), 1187 (w), 1121 (s), 1036 (s), 1000 (m), 873 (s), 830 (s), 755 (s), 660 (m).

**Preparation of G<sub>4</sub>TSP-(acetone)<sub>2</sub>.** Slow diffusion of acetone vapor into an aqueous solution of G<sub>4</sub>TSP afforded needle-shaped crystals. Elemental anal. calcd for C<sub>26</sub>H<sub>44</sub>O<sub>14</sub>S<sub>4</sub>N<sub>12</sub>: C 35.62, H 5.02, N 19.18. Found: C 36.04, H 4.85, N 19.34. IR: 3382 (w), 3196 (w), 1669 (s), 1562 (m), 1196 (m), 1119 (s), 1023 (s), 994 (s), 747 (s), 663 (s), 589 (m).

**Preparation of G<sub>6</sub>HSMB.** Slow evaporation of an aqueous solution of G<sub>6</sub>HSMB afforded well-defined plate-like crystals. Elemental anal. calcd for C<sub>18</sub>H<sub>48</sub>O<sub>18</sub>S<sub>6</sub>N<sub>18</sub>: C 21.68, H 4.85, N 25.29. Found: C 21.48, H 4.88, N 25.15. IR: 3328 (s), 3194 (s), 1669 (s), 1581 (m), 1257 (w), 1195 (s), 1137 (s), 1034 (s), 950 (w), 797 (w), 765 (w), 727 (w), 664 (w).

**Preparation of G<sub>6</sub>HSPB.** Slow evaporation of an anhydrous methanol solution of G<sub>6</sub>HSPB afforded needle-shaped crystals. Satisfactory element analysis cannot be obtained for this compound. IR: 3736 (w), 3420 (s), 3171 (m), 2790 (w), 1946 (w), 1665 (vs), 1470 (w), 1385 (m), 1183 (s), 1118 (m), 1036 (s), 1011 (s), 847 (w), 669 (vs), 560 (w), 431 (w).

**Crystallography.** Data using Mo radiation were collected on a Bruker SMART APEX II diffractometer equipped with a CCD detector and operated at 1500W power (50KV, 30 mA) to generate Mo K $\alpha$  radiation ( $\lambda = 0.71073 \text{ \AA}$ ), which is graphite monochromated and MonoCap-collimated.<sup>31</sup> The crystal was mounted on an 0.3 mm 20  $\mu\text{m}$ -thick Nylon Cryoloop (Hampton Research) with immersion oil of type B (Cargille Laboratories) frozen at 100 K with an Oxford Cryosystems 700 plus Cooler.

Preliminary lattice parameters and orientation matrices were obtained from three sets of frames.<sup>32</sup> Then full data were collected using the  $\omega$  scan method with the frame width of 0.5.<sup>33</sup> Data were processed with the SAINT+ program<sup>34</sup> for reduction and cell refinement. Multiscan absorption corrections were applied by using the SADABS program for area detector. All structures were solved by the direct method (SHELXS-97) and refined on F<sup>2</sup> (SHELXL-97).<sup>35</sup> Non-hydrogen atoms were refined with anisotropic displacement parameters, and hydrogen atoms on carbons were placed in idealized positions (C–H = 0.93 or 0.96  $\text{\AA}$ ) and included as riding with Uiso(H) = 1.2 or 1.5 Ueq(non-H). The PLATON/SQUEEZE<sup>21</sup> procedure was applied to handle the heavily disordered components (ions and solvents) in the voids of the frameworks.

## ASSOCIATED CONTENT

### Supporting Information

Experimental details, characterization, and crystallographic data in CIF format. This material is available free of charge via the Internet at <http://pubs.acs.org>.

## AUTHOR INFORMATION

### Corresponding Author

\*mdw3@nyu.edu

### Present Addresses

<sup>†</sup>School of Chemistry and Environment, Beihang University, Beijing, 100191, China

#Environmental Energy Technologies Division, Lawrence Berkeley National Laboratory, Berkeley, California 94720, United States

### Notes

The authors declare no competing financial interest.

### ACKNOWLEDGMENTS

The authors acknowledge the support of the National Science Foundation through DMR-1308677, the NSF CRIF Program (CHE-0840277), and the NSF MRSEC Program (DMR-0820341) for shared facilities.

### REFERENCES

- (1) (a) Bengen, M. F. *Experientia* **1949**, *5*, 200. (b) Hollingsworth, M. D.; Brown, M. E.; Hillier, A. C.; Santarsiero, B. D.; Chaney, J. D. *Science* **1996**, *273*, 1355.
- (2) Hoss, R.; König, O.; Kramer-Hoss, V.; Berger, U.; Rogin, P.; Hulliger, J. *Angew. Chem., Int. Ed.* **1996**, *35*, 1664.
- (3) Hertzsch, T.; Budde, F.; Weber, E.; Hulliger, J. *Angew. Chem.* **2002**, *114*, 2385.
- (4) Yang, J.; Dewal, M. B.; Shimizu, L. S. *J. Am. Chem. Soc.* **2006**, *128*, 8122.
- (5) Görbitz, C. H. *Acta Crystallogr., Sect. B: Struct. Sci.* **2002**, *58*, 849.
- (6) Comotti, A.; Bracco, S.; Distefano, G.; Sozzani, P. *Chem. Commun.* **2009**, 284.
- (7) Yang, J.; Dewal, M. B.; Profeta, S.; Smith, M. D.; Li, Y. Y.; Shimizu, L. S. *J. Am. Chem. Soc.* **2008**, *130*, 612.
- (8) (a) McKeown, N. B. *J. Mater. Chem.* **2010**, *20*, 10588. (b) Mastalerz, M. *Chem.—Eur. J.* **2012**, *18*, 10082. (c) Holst, J. R.; Trewin, A.; Cooper, A. I. *Nat. Chem.* **2010**, *2*, 915. (d) Lim, S.; Kim, H.; Selvapalam, N.; Kim, K.-J.; Cho, S. J.; Seo, G.; Kim, K. *Angew. Chem., Int. Ed.* **2008**, *47*, 3352. (e) Sozzani, P.; Bracco, S.; Comotti, A.; Ferretti, L.; Simonutti, R. *Angew. Chem., Int. Ed.* **2005**, *44*, 1816.
- (9) Reichenbacher, K.; Neels, A.; Stoeckli-Evans, H.; Balasubramanian, P.; Müller, K.; Matsuo, Y.; Nakamura, E.; Weber, E.; Hulliger, J. *Cryst. Growth Des.* **2007**, *7*, 1399.
- (10) Russell, V. A.; Etter, M. C.; Ward, M. D. *J. Am. Chem. Soc.* **1994**, *116*, 1941.
- (11) Russell, V. A.; Evans, C. C.; Li, W.; Ward, M. D. *Science* **1997**, *276*, 575.
- (12) Swift, J. A.; Reynolds, A. M.; Ward, M. D. *Chem. Mater.* **1998**, *10*, 4159.
- (13) Evans, C. C.; Sukarto, L.; Ward, M. D. *J. Am. Chem. Soc.* **1999**, *121*, 320.
- (14) Holman, K. T.; Pivovar, A. M.; Swift, J. A.; Ward, M. D. *Acc. Chem. Res.* **2001**, *34*, 107.
- (15) Burke, N. J.; Burrows, A. D.; Mahon, M. F.; Teat, S. J. *CrystEngComm* **2004**, *6*, 429.
- (16) Dumitrescu, D.; Legrand, Y.-M.; Dumitrescu, F.; Barboiu, M.; van der Lee, A. *Cryst. Growth Des.* **2012**, *12*, 4258.
- (17) Horner, M. J.; Holman, K. T.; Ward, M. D. *Angew. Chem., Int. Ed.* **2001**, *40*, 4045.
- (18) Comotti, A.; Bracco, S.; Sozzani, P.; Hawxwell, S. M.; Hu, C. H.; Ward, M. D. *Cryst. Growth Des.* **2009**, *9*, 2999.
- (19) Ajayan, P. M. *Chem. Rev.* **1999**, *99*, 1787.
- (20) Yang, C. I.; Song, Y. T.; Yeh, Y. J.; Liu, Y. H.; Tseng, T. W.; Lu, K. L. *CrystEngComm* **2011**, *13*, 2678.
- (21) Spek, A. L. *J. Appl. Cryst.* **2003**, *36*, 7.
- (22) Xiao, W.; Hu, C.; Ward, M. D. *J. Am. Chem. Soc.* **2014**, *136*, 14200.
- (23) Soegiarto, A.; Comotti, A.; Ward, M. D. *J. Am. Chem. Soc.* **2010**, *132*, 14603.
- (24) Liu, Y. Z.; Hu, C. H.; Comotti, A.; Ward, M. D. *Science* **2011**, *333*, 436.
- (25) Suter, C. M.; Harrington, G. A. *J. Am. Chem. Soc.* **1937**, *59*, 2575.
- (26) Schneider, H. J.; Schiestel, T.; Zimmermann, P. *J. Am. Chem. Soc.* **1992**, *114*, 7698.
- (27) Mahmoudkhani, A. H.; Cote, A. P.; Shimizu, G. K. H. *Chem. Commun.* **2004**, 2678.
- (28) Dalrymple, S. A.; Parvez, M.; Shimizu, G. K. H. *Inorg. Chem.* **2002**, *41*, 6986.
- (29) Dalrymple, S. A.; Shimizu, G. K. H. *Supramol. Chem.* **2003**, *15*, 591.
- (30) Tugcu, N.; Park, S. K.; Moore, J. A.; Cramer, S. M. *Ind. Eng. Chem. Res.* **2002**, *41*, 6482.
- (31) *APEXII, Program for Bruker CCD X-ray Diffractometer Control* (version 2009.5); Bruker AXS, Inc.: Madison, WI, 2009.
- (32) *SAINT+, Program for reduction of data collected on a Bruker CCD area detector diffractometer* (version 7.60A); Bruker AXS, Inc.: Madison, WI, 2008.
- (33) Sheldrick, G. M. *SADABS, Program for empirical absorption correction of area-detector data*; Universität Göttingen: Göttingen, Germany, 2008.
- (34) Sheldrick, G. M. *SHELXS-97, Program for solution of crystal structures*; Universität Göttingen: Göttingen, Germany, 1997.
- (35) Sheldrick, G. M. *SHELXL-97, Program for refinement of crystal structures*; Universität Göttingen: Göttingen, Germany, 1997.